Annual Review of Nuclear and Particle Science

Flavor Phenomenology of Light Dark Sectors

Jorge Martin Camalich[1] and Robert Ziegler[2]

[1]Instituto de Astrofísica de Canarias y Departamento de Astrofísica, Universidad de La Laguna, La Laguna, Tenerife, Spain; email: jcamalich@iac.es

[2]Institute for Theoretical Particle Physics, Karlsruhe Institute of Technology, Karlsruhe, Germany

Annu. Rev. Nucl. Part. Sci. 2025. 75:223–46

First published as a Review in Advance on June 23, 2025

The *Annual Review of Nuclear and Particle Science* is online at nucl.annualreviews.org

https://doi.org/10.1146/annurev-nucl-121423-100931

Keywords

light dark matter, dark sectors, axions, flavor physics, flavor-changing neutral currents

Abstract

The dark sector offers a compelling theoretical framework for addressing the nature of dark matter while potentially solving other fundamental problems in physics. This review focuses on light dark-flavored sector models, in which the flavor structure of the interactions with the Standard Model is nontrivial and distinguishes among different fermion families. Such scenarios feature flavor violation that leads to unique experimental signatures, such as flavor-changing neutral current decays of heavy hadrons (kaons, D and B mesons, baryons) and leptons (muons and taus) with missing energy carried away by light dark-sector particles. In this article, we review their motivation, summarize current constraints, highlight discovery opportunities in ongoing and future flavor experiments, and discuss implications for astrophysics and cosmology.

Contents

1. INTRODUCTION

Despite the remarkable success of the Standard Model of particle physics (SM) and the standard cosmological model (ΛCDM), several fundamental questions remain unanswered: What is the nature of dark matter (DM) and dark energy? What caused the matter–antimatter asymmetry observed in the Universe? Why is charge parity conserved in the strong interactions? What is the source of flavor, and why does matter exhibit three distinct families? These and other questions continue to drive extensive theoretical and experimental efforts aiming to uncovering new laws of nature and potentially reveal entirely new sectors of constituents that can address these foundational problems.

A general theoretical framework that primarily addresses the nature of DM, while potentially solving other fundamental questions, is the dark sector. The dark sector can describe a minimal scenario involving a new particle, such as the QCD axion, weakly coupled with the SM and playing the role of DM. More broadly, it often refers to an extended sector comprising several new particles and interactions. Over the past decade, a surge of theoretical activity has aimed to characterize these dark sectors, especially by exploring their connections to other fundamental puzzles, and has given rise to novel ideas for their detection and potential discovery through experiments and observations (1–4).

In this review, we focus on a specific aspect of the dark sector: the flavor structure of its interactions with the SM. In particular, we examine cases where this flavor structure is nontrivial (i.e., not proportional to the identity matrix) in generation space but where the interactions and couplings with the dark sector distinguish among the fermion families of the SM. Such scenarios naturally arise in dark sectors intertwined with solutions to the SM flavor puzzle or baryogenesis. The prototypical example is the QCD axion with nondiagonal flavor couplings (5), which simultaneously addresses the DM, strong *CP*, and flavor problems. Other examples include the dark photon (6, 7) and dark baryons (8).

One of the most significant implications of these dark-flavored sectors is their potential to induce flavor-violating transitions among SM fermions. Furthermore, if the dark-sector particle mediating these transitions is sufficiently light, then it can be produced in heavy flavor and detected

through missing energy signatures (9). This phenomenology opens up a wide range of unexplored avenues for discovery in flavor experiments, focused on the decays of heavy-flavored hadrons (e.g., kaons, D or B mesons, and baryons) or heavy leptons (e.g., muons, taus). These opportunities are especially timely because flavor physics is currently experiencing a golden age in experimental precision and reach. This includes multipurpose experiments in flavor factories such as LHCb (10), Belle II (11), and BESIII (12), as well as specialized experiments such as NA62 (13), KOTO (14), and MEG-II (15) that target specific rare decays with exceptional sensitivity.

In this article, we review the phenomenology of light dark-flavored sectors, where "light" refers to particles that are effectively massless or have negligible masses relative to the energy scales of interest (see Section 2). We focus on the experimental signatures associated with kinematic configurations of decays involving missing energy and provide an overview of the current constraints on these models derived from flavor physics experiments (see Section 3). Furthermore, we explore the sensitivity and discovery potential of current and future searches specifically designed to target these experimental signatures (see Section 4). Finally, we review the consequences of dark-flavored sectors in astrophysics and cosmology, with the corresponding limits derived on their interactions (see Sections 5 and 6, respectively).

2. SETUP AND MOTIVATION

We explore extensions of the SM by introducing neutral bosonic particles with masses significantly below the GeV scale. Specifically, we consider the addition of either a new scalar particle a with mass m_a or a new light vector boson V'_μ with mass $m_{V'}$. We start from a basis in which these new states are orthogonal to the SM states, that is, where a possible kinetic mixing between the photon and the light vector boson has already been diagonalized.

Below the electroweak (EW) scale, the interactions of the new states with the SM fermions can be systematically described through an effective field theory (EFT) approach by introducing the most general set of operators that respect the unbroken part of the SM gauge group, $SU(3)_c \times U(1)_{\rm em}$. Here, we focus exclusively on flavor-violating interactions, written without loss of generality in the fermion mass basis. The leading-order interactions, in EFT power counting, of the new bosons are described by the following operators:

$$\mathcal{L}_{\rm scalar} = -\frac{i}{\Lambda} a\, \overline{f}_i \left[(m_i - m_j)\mathbb{C}^{\rm S}_{ij} + (m_i + m_j)\mathbb{C}^{\rm S5}_{ij}\gamma_5 \right] f_j, \qquad 1.$$

$$\mathcal{L}_{\rm vector} = \frac{m_{V'}}{\Lambda} V'_\mu\, \overline{f}_i \gamma^\mu \left(\mathbb{C}^{\rm V}_{ij} + \mathbb{C}^{\rm V5}_{ij}\gamma_5 \right) f_j, \qquad 2.$$

where $i \neq j$ denote SM quark or lepton flavors and all couplings are Hermitian matrices in flavor space [e.g., $(\mathbb{C}^{\rm S}_{ij})^* = \mathbb{C}^{\rm S}_{ji}$].

The couplings are normalized with respect to a UV scale Λ. For the scalar case, we choose a convenient prefactor, as discussed below in Section 2.1. Note that, above the EW scale, the couplings in Equation 1 are not $SU(2)_L$ invariant and must involve a single power of the EW breaking scale. Furthermore, flavor-violating currents coupled to a vector boson (Equation 2) are not conserved and must be proportional to at least one power of the $U(1)'$ breaking scale, which is the vector mass $m_{V'}$, upon including the dark gauge coupling (for more details, see Reference 16). This normalization also ensures finite amplitudes in the $m_{V'} \to 0$ limit, which correspond to the amplitudes with the associated Goldstone bosons as initial or final states. Indeed, in this limit, the longitudinal polarization dominates according to the Goldstone boson equivalence theorem. With the replacement $V'_\mu \to \partial_\mu a / m'_V$ and integrating by parts, one recovers the scalar interactions

in Equation 1, thereby identifying $\mathbb{C}^{S}_{ij} = \mathbb{C}^{V}_{ij}$ and $\mathbb{C}^{S5}_{ij} = \mathbb{C}^{V5}_{ij}$. Doing so also justifies the chosen fermion mass normalization factors for scalar couplings in Equation 1.

Genuinely new interactions of a very light vector boson can be described by flavor-violating dipole interactions, as given by (e.g., 17)

$$\mathcal{L}_{\text{dipole}} = \frac{1}{\Lambda} V'_{\mu\nu}\, \overline{f}_i \sigma^{\mu\nu} \left(\mathbb{C}^{D}_{ij} + i\,\mathbb{C}^{D5}_{ij}\gamma_5\right) f_j, \qquad 3.$$

where $V'_{\mu\nu} = \partial_\mu V'_\nu - \partial_\nu V'_\mu$, $\sigma^{\mu\nu} = i/2\,[\gamma^\mu, \gamma^\nu]$, and the dipole couplings $\mathbb{C}^{D}_{ij}$ and $\mathbb{C}^{D5}_{ij}$ are Hermitian matrices in flavor space. Note that this operator is naturally of dimension six if the mass scale of the associated UV physics is significantly larger than the EW scale, as required by $SU(2)_L$ invariance (7). In this case, the UV scale Λ should be replaced by Λ^2/v, where $v = 174$ GeV is the Higgs field vacuum expectation value.

We assume that the other possible interactions with the SM particles, particularly the flavor-diagonal couplings to fermions, are sufficiently small to ensure that the new bosons remain stable on collider scales. Under this assumption, limits on the flavor-violating couplings of dark bosons described by the interactions

$$\mathcal{L}_{\text{int}} = \mathcal{L}_{\text{scalar}} + \mathcal{L}_{\text{vector}} + \mathcal{L}_{\text{dipole}} \qquad 4.$$

with Equations 1–3 can be derived from hadronic and leptonic decays with missing energy in the final state. These constraints also apply when the dark boson is unstable but promptly decays into stable invisible particles, such as dark fermions or neutrinos.

The scenarios described by the above Lagrangians can be well-motivated in SM extensions that are capable of (possibly simultaneously) explaining some of the problems and shortcomings of the SM, such as the existence of DM (e.g., 4), the absence of *CP* violation in strong interactions (e.g., 18), and the flavor puzzle (e.g., 19). In the following subsections, we briefly discuss some of these frameworks.

2.1. Axion Dark Matter

Arguably, the most prominent motivation for the above setup is the QCD axion (20, 21), which emerges as a low-energy remnant of the Peccei–Quinn (PQ) solution to the strong *CP* problem (22, 23), namely the observed absence of *CP* violation in strong interactions. As a pseudo-Goldstone boson, the QCD axion mass is protected by the nonlinearly realized PQ symmetry, which by definition is broken primarily by QCD instantons. Consequently, the QCD axion acquires a mass given by (24)

$$m_a = 5.7\ \text{meV} \left(\frac{10^9\ \text{GeV}}{f_a}\right), \qquad 5.$$

where f_a is the axion decay constant. This constant must lie well above the EW scale for phenomenological reasons, leading to a typical axion mass well below the eV scale (18). Additionally, the QCD axion is an excellent cold DM candidate over large regions of parameter space, when produced in the early Universe via the misalignment mechanism (25–27).

The most general couplings of the axion to the SM fermions can be written as

$$\mathcal{L}_a = \frac{\partial_\mu a}{2 f_a}\, \overline{f}_i \gamma^\mu \left(C^{V}_{ij} + C^{A}_{ij}\gamma_5\right) f_j, \qquad 6.$$

where $C^{V,A}_{ij}$ are Hermitian matrices in flavor space. This Lagrangian can be mapped to the couplings in Equation 1 by fermion field redefinitions, which, apart from anomalous couplings to the

SM gauge bosons, give rise to the identifications

$$\frac{\mathbb{C}^{\mathrm{S}}_{ij}}{\Lambda} = \frac{C^{V}_{ij}}{2f_a}, \qquad \frac{\mathbb{C}^{\mathrm{S5}}_{ij}}{\Lambda} = \frac{C^{A}_{ij}}{2f_a}. \qquad 7.$$

The flavor-violating couplings $C^{V,A}_{i\neq j}$ are determined by rotating the flavor-diagonal PQ charge matrices into the fermion mass basis (for details, see Reference 28). In common QCD axion benchmark models, flavor alignment is realized either because the PQ charges of the SM fermions vanish (KSVZ models; 29, 30) or because PQ charges are taken to be flavor universal (standard DFSZ models; 31, 32). However, the PQ charges in the DFSZ models do not have to be flavor universal and may constitute a new source of flavor violation beyond the SM Yukawas (33–35). In such scenarios, the size of flavor-violating axion couplings depends on the magnitude of the flavor misalignments parameterized by the unitary matrices that diagonalize the SM Yukawas. Thus, in the absence of a theory of flavor, these rotations are simply described by a variety of new free parameters, which can be suitably chosen to realize an arbitrary pattern of flavor structures $C^{V,A}_{ij}$. Particular flavor patterns have been employed to, for instance, suppress the axion couplings to nucleons (36, 37) and address stellar cooling anomalies (38), possibly correlated with low-energy signals from the extra DFSZ Higgs doublet (39).

Particularly well-motivated and predictive scenarios emerge when the PQ symmetry is identified with a flavor symmetry that addresses the SM flavor puzzle (5, 40–43). For instance, in the simplest realization, the PQ symmetry is identified with a $U(1)_F$ Froggatt–Nielsen symmetry (44), which necessarily possesses a QCD anomaly (45, 46). This setup allows one to predict flavor-violating axion couplings up to model-dependent $\mathcal{O}(1)$ coefficients (42, 43). Specifically, it determines the most phenomenologically relevant coupling, C^{V}_{sd} (see Section 3), to be on the order of the Cabibbo angle, $C^{V}_{sd} \sim V_{us} \sim 0.2$. Stronger suppression of light quark transitions occurs in models with nonabelian flavor symmetries; for example, in $U(2)$ models, $C^{V}_{sd} \sim V_{td}V_{ts} \sim 10^{-4}$ (47). For the lepton sector, several models have been presented (48) that can naturally yield large lepton flavor violation (LFV), for example, with couplings $C^{V}_{\mu e} \sim V_{us} \sim 0.2$ or $C^{V}_{\mu e} \sim \sqrt{m_e/m_\mu} \sim 0.1$.

Note that, even in scenarios with flavor alignment, renormalization group running induces flavor violation proportional to the CKM angles (28, 49–51). That leads to strongly suppressed off-diagonal couplings, such as $C^{V}_{sd} \sim y_t^2/(16\pi^2)V_{td}V_{ts}C^{V}_{tt} \log \Lambda_{\mathrm{UV}}/\Lambda_{\mathrm{IR}} \sim 10^{-5}$, which are phenomenologically irrelevant for axion masses $m_a \ll$ keV, since astrophysical constraints on the flavor-diagonal couplings yield significantly stronger constraints (see Section 5).

If there are substantial sources of explicit PQ breaking beyond QCD instantons, typically the axion acquires a large mass and does not solve the strong *CP* problem,[1] and it is called an axion-like particle (ALP). Nevertheless, the ALP can still be a good DM candidate, provided that its lifetime is sufficiently long. ALPs can be produced in the early Universe by, for example, misalignment, thermal freeze-in (52), or parametric resonance (53). In general, such ALPs can also have the same flavor-violating couplings in Equation 6 as the QCD axion and, thus, are constrained in exactly the same way, provided that their mass is below the experimental resolution. A flavor-violating ALP also has the same theoretical motivation as the QCD axion, possibly being a pseudo-Goldstone boson associated with global flavor symmetries that address the Yukawa hierarchies, such as the "familon" (5), "flaxion" (42), "axiflavon" (43), or "Froggatt–Nielsen ALP" (54). Such a light ALP could arise from the spontaneous breaking of other global symmetries like baryon number (55) or, more prominently, lepton number, in which case it is called the "majoron" (56, 57). In this

[1]Unless one employs further model building with, for instance, new gauge sectors confining at large energies with aligned vacuum angles (for an overview of such models, see Reference 18).

scenario, large LFV couplings can be connected to the origin of neutrino masses in low-energy seesaw models (for an example, see Reference 48). A light scalar with flavor-violating couplings could also be motivated as one of the moduli predicted by superstring compactifications (58). It might be related to modular flavor symmetries (59), which have been employed for the flavor puzzle (60) or to solve the strong *CP* problem with spontaneous *CP* violation (61).

2.2. Light Vector Dark Matter

A light vector particle is also a viable DM candidate (62, 63) that can be produced in the early Universe by, for example, misalignment, thermal freeze-in, or parametric resonance, as for ALPs. These particles are often referred to in the literature as dark photons, hidden photons, or dark Z's. A dark photon usually refers to a vector that inherits all couplings to SM fermions from mixing with the photon and thus couples mainly to diagonal flavors. Instead, general light vectors couple to fermions when the latter carry nontrivial charges under the dark gauge group, which generically induces flavor-violating couplings of the form in Equation 2 when the charges are not universal (for more details, see Reference 16). This scenario is particularly well-motivated when the dark gauge group is identified with an anomaly-free flavor symmetry group that shapes the structure of Yukawa matrices (e.g., 64–66) or flavor-nonuniversal charges such as $U(1)_{L_i-L_j}$ (67, 68). While the breaking scale of the gauge group must typically be much larger than the EW scale (for a counterexample, see Reference 69), the associated massive gauge boson can be light enough for our purposes if the gauge coupling is sufficiently small. Instead, dipole couplings of the form in Equation 3 can arise in models where the dark photon is extremely light, so that kinetic mixing is suppressed and the dominant couplings to SM fermions occur through higher-dimensional operators (e.g., 70).

2.3. Axion and Vector Portals

The flavor phenomenology of the couplings in Equation 4 cannot distinguish between bosons that are dark and bosons that promptly decay into dark particles. These could be part of a larger theoretical structure (the dark sector) to which the bosons in Equation 4 would merely act as mediators, or "portals" (71–73). An appealing theoretical feature is that these lighter dark particles can easily be cosmologically stable as a result of some conserved quantum number in the dark sector, such as the dark fermion number. A new phenomenological aspect is that the (typically long-lived) bosonic mediator could also decay into SM particles. The light mediator can then be created on-shell from decays of, for instance, B or D mesons (copiously produced at hadron colliders) and may travel macroscopic distances before decaying visibly within, say, the SHiP detector (74, 75), located at the SPS, or dedicated forward detectors at the LHC, such as FASER (76, 77). This possibility gives rise to a rich phenomenology that correlates signals at flavor factories like NA62 and Belle II with essentially background-free searches at next-generation beam-dump experiments (78, 79).

3. CURRENT LIMITS

The couplings in Equation 4 give rise to two-body decays of SM particles, such as $K \to \pi X$ or $\mu \to eX$, where X denotes a dark scalar or dark vector boson; dark vector bosons would manifest as missing energy in a laboratory experiment. Thus, the experimental signature resembles SM decays involving a neutrino pair, but with a monochromatic visible particle. Its energy is essentially determined by the mass of the invisible particle, which we assume to be approximately massless (i.e., with a mass below the experimental resolution).

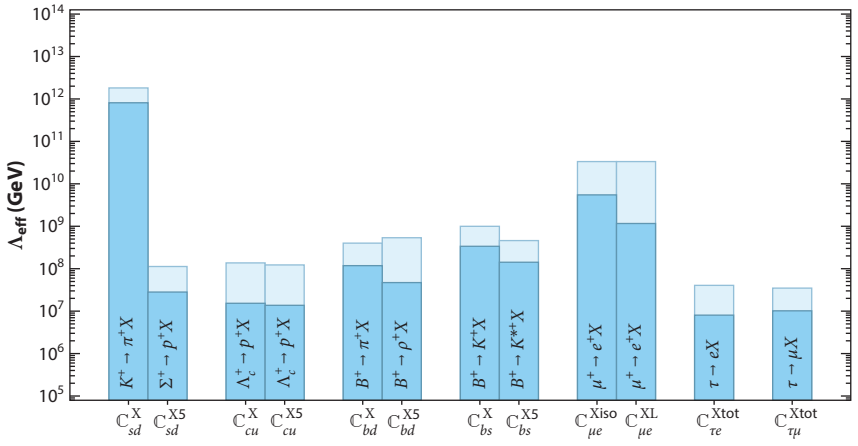

Figure 1

Present limits on scalar and vector couplings for a massless dark boson. For a given quark flavor transition $i \to j$ and chirality structure X,X5, the bound is $\Lambda_{\rm eff} = \Lambda/|\mathbb{C}^{\rm S,S5}_{ij}|$ for massless scalars (see Equation 1), $\Lambda_{\rm eff} = \Lambda/|\mathbb{C}^{V,V5}_{ij}|$ for massless vectors (see Equation 2), and $\Lambda_{\rm eff} = 2f_a/|\mathbb{C}^{V,A}_{ij}|$ for derivative axion couplings (see Equation 6). For lepton transitions, $\Lambda_{\rm eff} = \Lambda/|\mathbb{C}^{Xa}_{ij}|$ with $\mathbb{C}^{\rm Xtot}_{ij} = \sqrt{|\mathbb{C}^{\rm X}_{ij}|^2 + |\mathbb{C}^{\rm X5}_{ij}|^2}$, $\mathbb{C}^{\rm Xiso}_{ij} = \mathbb{C}^{\rm X}_{ij}$ or $\mathbb{C}^{\rm X5}_{ij}$, and $\mathbb{C}^{\rm XL}_{ij} = \mathbb{C}^{\rm Xtot}_{ij}|_{\mathbb{C}^{\rm X}_{ij} = -\mathbb{C}^{\rm X5}_{ij}}$ for massless scalars and vectors, and similarly for derivative couplings. Dark bars represent present limits, while light bars represent expected future constraints.

The flavor-violating decay rate of a particle with mass m into light bosons scales as $m^3/\Lambda^2_{\rm UV}$ because it arises from dimension-five operators. In contrast, a flavor-changing SM decay rate scales as $\propto m^5 G_{\rm F}^2$, with possible contributions from new heavy particles scaling as $\propto m^5/\Lambda^4_{\rm UV}$, because both arise from dimension-six operators. Furthermore, SM amplitudes can be reduced by additional small factors due to chirality, loop effects, phase space, and/or CKM matrix elements, leading to a significant suppression relative to the two-body decay rate. Consequently, two-body missing energy searches can have an enormous sensitivity to the flavor-violating couplings in Equation 4. For example, the ratio of muon decay rates is given by

$$\frac{\Gamma(\mu \to eX)}{\Gamma(\mu \to e\nu\overline{\nu})} \approx \frac{m_\mu^3(|\mathbb{C}^{\rm X}_{\mu e}|^2 + |\mathbb{C}^{\rm X5}_{\mu e}|^2)/(16\pi\Lambda^2)}{m_\mu^5 G_{\rm F}^2/(192\pi^3)} = \left(\frac{9 \times 10^6\ {\rm GeV}}{\Lambda^{\rm X}_{\mu e}}\right)^2, \qquad 8.$$

where we neglect the electron mass, defined as $\Lambda^{\rm X}_{\mu e} = \Lambda/\sqrt{|\mathbb{C}^{\rm X}_{\mu e}|^2 + |\mathbb{C}^{\rm X5}_{\mu e}|^2}$, and X denotes either a massless dark scalar (for which $\mathbb{C}^{\rm X,X5}_{\mu e} = \mathbb{C}^{\rm S,S5}_{\mu e}$) or a massless dark vector (for which $\mathbb{C}^{\rm X,X5}_{\mu e} = \mathbb{C}^{\rm V,V5}_{\mu e}$). This means that the muon lifetime alone already sets a bound on the UV scale of order 10^7 GeV.

Dedicated searches for two-body decays with missing energy yield limits that are even more stringent. **Figures 1** and **2** display the best current limits[2] on the couplings to massless dark bosons from laboratory experiments for each flavor transition (see also **Tables 1** and **2**). The figures report and update previous limits for dark scalars (28, 48, 51, 80–82), dark vectors (16, 83, 84), and massless dark vectors with dipole couplings (17, 70, 85–88).

In the following subsections, we discuss the experimental origin of these bounds in more detail, considering the couplings to quarks and to leptons separately. This separation is useful because in

[2]For simplicity, for hadron decays we neglect the systematic errors on the associated form factors, which are nonetheless small for the decays of interest and have no major impact on the bounds.

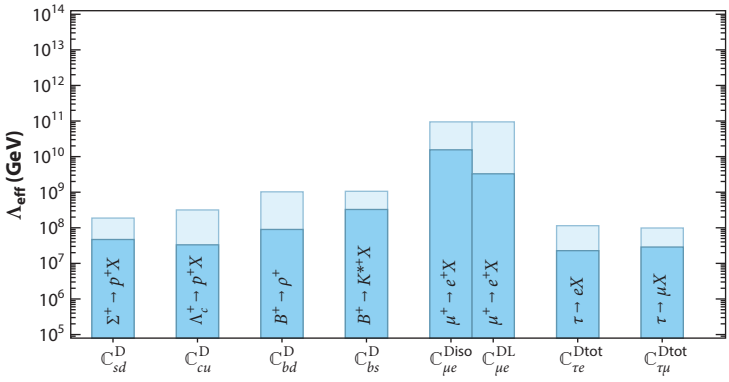

Figure 2

Present limits on dipole couplings for a massless dark vector. For a given quark flavor transition $i \to j$, the bound is independent of the chiral structure $\Lambda_{\rm eff} = \Lambda/|\mathbb{C}^{\rm D,D5}_{ij}|$. For lepton transitions, $\Lambda_{\rm eff} = \Lambda/|\mathbb{C}^{Da}_{ij}|$ with $\mathbb{C}^{\rm Diso}_{ij} = \mathbb{C}^{\rm D}_{ij}$ or $\mathbb{C}^{\rm D5}_{ij}$, $\mathbb{C}^{\rm Dtot}_{ij} = \sqrt{|\mathbb{C}^{\rm D}_{ij}|^2 + |\mathbb{C}^{\rm D5}_{ij}|^2}$, and $\mathbb{C}^{\rm DL}_{ij} = \mathbb{C}^{\rm Dtot}_{ij}|_{\mathbb{C}^{\rm D}_{ij} = -\mathbb{C}^{\rm D5}_{ij}}$. Dark bars represent present limits, while light bars represent expected future constraints.

the quark sector the strongest limits typically come from pseudoscalar meson decays, which are sensitive to the chiral structure in Equation 4, whereas in the lepton sector the total decay rates do not depend on chirality. However, at least in the case of muons, one can rely on polarization, which enables control of the different couplings via the angular distribution of the final-state lepton. In contrast to the quark sector, the SM background is huge; thus, it is convenient to constrain the couplings according to whether or not the chiral structure is aligned to the SM (i.e., left-handed couplings with $\mathbb{C}^{\rm X}_{ij} = -\mathbb{C}^{\rm X5}_{ij}$). For simplicity, we restrict the discussion of misaligned structures to isotropic decays, corresponding to couplings with either $\mathbb{C}^{\rm X}_{ij} = 0$ or $\mathbb{C}^{\rm X5}_{ij} = 0$.

3.1. Quark Sector

In the quark sector, the strongest constraints typically arise from laboratory searches for two-body decays of pseudoscalar mesons and baryons with an invisible scalar or vector particle in the final state. These decay rates scale with the couplings according to

$$\Gamma_{P\to P'X} \propto |\mathbb{C}^{\rm X}_{ij}|^2, \qquad \Gamma_{P\to VX} \propto |\mathbb{C}^{\rm X5}_{ij}|^2, \qquad \Gamma_{B\to B'X} \propto f_1^2 |\mathbb{C}^{\rm X}_{ij}|^2 + g_1^2 |\mathbb{C}^{\rm X5}_{ij}|^2, \qquad 9.$$

Table 1 Present and expected laboratory limits on effective couplings of massless dark scalars and vectors[a]

	$\mathbb{C}^{\rm X}_{sd}$	$\mathbb{C}^{\rm X5}_{sd}$	$\mathbb{C}^{\rm X}_{cu}$	$\mathbb{C}^{\rm X5}_{cu}$
$\Lambda_{\rm eff}$	8.1×10^{11} (89)	2.8×10^{7} (90)	1.5×10^{7} (91)	1.4×10^{7} (91)
$\Lambda^{\rm proj}_{\rm eff}$	1.8×10^{12} (NA62)	1.1×10^{8} (STCF)	1.4×10^{8} (STCF)	1.2×10^{8} (STCF)
	$\mathbb{C}^{\rm X}_{bd}$	$\mathbb{C}^{\rm X5}_{bd}$	$\mathbb{C}^{\rm X}_{bs}$	$\mathbb{C}^{\rm X5}_{bs}$
$\Lambda_{\rm eff}$	1.2×10^{8} (28, 92)	4.7×10^{7} (93, 94)	3.4×10^{8} (95–97)	1.4×10^{8} (96, 97)
$\Lambda^{\rm proj}_{\rm eff}$	4.0×10^{8} (Belle II)	5.4×10^{8} (Belle II)	1.0×10^{9} (Belle II)	4.6×10^{8} (Belle II)
	$\mathbb{C}^{\rm Xiso}_{\mu e}$	$\mathbb{C}^{\rm XL}_{\mu e}$	$\mathbb{C}^{\rm Xtot}_{\tau e}$	$\mathbb{C}^{\rm Xtot}_{\tau \mu}$
$\Lambda_{\rm eff}$	5.5×10^{9} (98)	1.2×10^{9} (99)	8.0×10^{6} (100)	1.0×10^{7} (100)
$\Lambda^{\rm proj}_{\rm eff}$	3.3×10^{10} (Mu3e)	3.3×10^{10} (Mu3e)	4.0×10^{7} (Belle II)	3.5×10^{7} (Belle II)

[a] Values are in units of GeV. The notation is the same as in **Figure 1**.

Table 2 Present and expected laboratory limits on effective dipole couplings of massless dark vectors[a]

	$\mathbb{C}^{\mathrm{D}}_{sd}$	$\mathbb{C}^{\mathrm{D}}_{cu}$	$\mathbb{C}^{\mathrm{D}}_{bd}$	$\mathbb{C}^{\mathrm{D}}_{bs}$
Λ_{eff}	4.7×10^7 (90)	3.3×10^7 (91)	9.0×10^7 (93, 94)	3.3×10^8 (96, 97)
$\Lambda^{\mathrm{proj}}_{\mathrm{eff}}$	1.9×10^8 (STCF)	3.2×10^8 (STCF)	1.0×10^9 (Belle II)	1.1×10^9 (Belle II)
	$\mathbb{C}^{\mathrm{Diso}}_{\mu e}$	$\mathbb{C}^{\mathrm{DL}}_{\mu e}$	$\mathbb{C}^{\mathrm{Dtot}}_{\tau e}$	$\mathbb{C}^{\mathrm{Dtot}}_{\tau \mu}$
Λ_{eff}	1.6×10^{10} (98)	3.3×10^9 (99)	2.3×10^7 (100)	2.9×10^7 (100)
$\Lambda^{\mathrm{proj}}_{\mathrm{eff}}$	9.5×10^{10} (Mu3e)	9.5×10^{10} (Mu3e)	1.1×10^8 (Belle II)	9.9×10^7 (Belle II)

[a]Values are in units of GeV. The notation is the same as in **Figure 2**.

where P and P' denote pseudoscalar mesons, V is a vector meson, B and B' are baryons, f_1 and g_1 are baryonic form factors, and we use the same notation for the couplings as above (for the complete expressions and a collection of the relevant form factors, see References 16 and 28).

To infer the limits in **Figures 1** and **2**, we compute these rates for a single coupling switched on at a time and compare them with the experimental limits on the various decays summarized in **Table 3**. Often, the experimental collaborations do not provide limits on two-body decays with missing energy; nevertheless, in some cases there is enough information to extract this bound from available data, as indicated in the table (for more details, see References 16 and 28). Of course, we would prefer these limits to be replaced by proper experimental analyses.

For $K \to \pi X$ and $\Sigma \to pX$, we use the experimental limits for invisible massless X reported by NA62 (89) and BESIII (90), respectively. Note that for the former decay a slightly stronger limit, $\mathrm{BR}(K^+ \to \pi^+ X) < 2.8 \times 10^{-11}$ (at 90% CL), was recently derived (102) by recasting the publicly available NA62 data set collected between 2016 and 2022. The stronger limit leads to a constraint on the effective coupling, $\mathbb{C}^{\mathrm{X}}_{\mathrm{sd}} > 1.1 \times 10^{12}$ GeV, that is tighter than the one shown in **Table 1**.

Table 3 Laboratory limits on the branching ratios of two-body meson, baryon, and lepton decays[a]

Decay	90%-CL limit	Reference(s)	Recast[b]
$\mathrm{BR}(K \to \pi X)$	5.0×10^{-11}	NA62 (89)	×
$\mathrm{BR}(\Sigma \to pX)$	3.2×10^{-5}	BESIII (90)[c]	×
$\mathrm{BR}(D \to \pi X)$	8.0×10^{-6}	CLEO (101)	✓ (28)
$\mathrm{BR}(\Lambda_c \to pX)$	8.0×10^{-5}	BESIII (91)	×
$\mathrm{BR}(B \to KX)$	7.0×10^{-6}	Belle II (95), BaBar (96)	✓ (97)
$\mathrm{BR}(B \to K^*X)$	4.2×10^{-5}	BaBar (96)	✓ (97)
$\mathrm{BR}(B \to \pi X)$	2.3×10^{-5}	BaBar (92)	✓ (28)
$\mathrm{BR}(B \to \rho X)$	3.9×10^{-4}	LEP (93)	✓ (94)
$\mathrm{BR}(\mu \to eX)_{\mathrm{iso}}$	2.6×10^{-6}	TRIUMF (98)	×
$\mathrm{BR}(\mu \to eX)_R$	2.5×10^{-6}	TRIUMF (98)	✓ (48)
$\mathrm{BR}(\mu \to eX)_L$	5.8×10^{-5}	TWIST (99)	×
$\mathrm{BR}(\tau \to \mu X)$	4.7×10^{-4}	Belle II (100)	×
$\mathrm{BR}(\tau \to eX)$	7.6×10^{-4}	Belle II (100)	×

[a]X denotes a massless invisible particle (i.e., any mass below the mass resolution of the experiments). For polarized muon decays, the limit depends on the angular distribution of the electron, denoted iso for isotropic decays, R for $\propto 1 + \cos\theta$, and L for $\propto 1 - \cos\theta$ (as in the Standard Model).

[b]In this column, checkmarks indicate that there was enough information to extract this bound from available data in the references shown.

[c]SN 1987A cooling constrains hyperon decays at the level of $\mathrm{BR}(\Lambda \to nX) \lesssim 8 \times 10^{-9}$ (88).

The recast of the $D \to \pi \nu \bar{\nu}$ decays requires a more detailed discussion. Reference 28 derived a bound on the two-body decay from a null search performed by CLEO (101) of the decay $D^+ \to \tau^+(\to \pi^+ \bar{\nu})\nu$ by recasting the bin in the pion spectrum corresponding to $m_X \approx 0$. Since then, two analyses by the BESIII Collaboration (103, 104) have reported observations of the $D^+ \to \tau^+(\to \pi^+ \bar{\nu})\nu$ decay mode. From the pion spectrum of the signal reported in these analyses, it is clear that a search for the two-body $D^+ \to \pi^+ X$ decay at BESIII (superseding the current CLEO recast) requires a careful treatment of the SM background from tau decays.

The BESIII Collaboration (12) has also reported a search for the three-body decay $D^0 \to \pi^0 \nu \bar{\nu}$ using 2.93 fb^{-1} of data (roughly one-seventh of the total luminosity planned to be collected at BESIII), obtaining the upper limit 2×10^{-4} at 90% CL for the branching fraction. If one takes this value as representative of the sensitivity achievable for $\text{BR}(D^0 \to \pi^0 X)$, the resulting limit would be considerably weaker than the recast of the CLEO data for the charged mode. This discussion highlights the importance of dedicated analyses of $D \to \pi X$ decays in both charged modes for a robust search for dark bosons in charmed meson decays.

Finally, in the context of probing *cu* couplings, the BESIII Collaboration (91) has searched for the baryonic two-body $\Lambda_c^+ \to pX$ decays using its complete data set. This search is especially relevant in light of the limitations discussed above with regard to current analyses of D meson decays, and it sets the best present limit on *cu* couplings. Slightly better limits can be obtained independently from $D^0 \to \omega X$ decays (105) by employing the theoretical predictions of Reference 106, which suggested this search.

For *bs* and *bd* couplings, no analyses of the invisible two-body decays of $B_{(s)}$ mesons or bottom baryons have been performed to date. Therefore, all of the existing limits are from recasts of searches of three-body decays into neutrinos (28, 94, 97). The upper limits on $B \to KX$, $B \to K^* X$, and $B \to \pi X$ use BaBar data (92, 96), while the upper limit on $B \to \rho X$ uses data from the ALEPH experiment at LEP (93). Only in the case of $B^+ \to K^+ X$ does the recast also use data from Belle II (95).

Three-body decays typically provide weaker constraints than two-body decays. For example, LHCb constraints on $B_{(s)} \to \mu\mu X$ cannot compete with Belle II limits from $B \to K^{(*)} X$ or $B \to \pi X$ and $B \to \rho X$ decays (107), while multihadron final states such as $B \to K\pi X$ are subject to larger theoretical uncertainties apart from experimental challenges. An exception is the kaon sector, where the corresponding $P \to VX$ decay mode is kinematically inaccessible ($m_\rho > m_K$) and an important bound stems from $K \to \pi\pi X$ decays. Experimentally, both $K^+ \to \pi^0\pi^+ X$ (108, 109) and $K_L \to \pi^0\pi^0 X$ (110) have been searched for. Theoretically, the decay rate into scalars can be predicted robustly using isospin symmetry and the form factors determined from the measurements of $K \to \pi\pi e\nu$ charge-current decays (28; see also 111–115). In fact, the strongest laboratory constraint on $\mathbb{C}_{sd}^{S5}$ stems from the OKA Collaboration's (109) upper limit on $K^+ \to \pi^0\pi^+ X$ (**Table 3**).[3] In principle, a similar analysis could be performed for decays involving a dark vector with dipole couplings. However, this scenario requires the computation of form factors in QCD, whereas current results rely only on approximate estimates derived from quark models (17).

Finally, neutral meson mixing, which yields the most stringent constraints on dimension-six SM EFT operators induced by heavy new physics (116), yields limits on flavor-violating couplings that are at most comparable to those obtained from two-body decays but are subject to uncertainties due to contributions from UV physics that are parametrically of the same order (28). For example, the radial mode in ALP models contributes to mixing amplitudes parametrically at the same level

[3]The decay mode $K_L \to \pi^0\pi^0 X$ in Reference 110 could nominally lead to a stronger bound, but the analysis does not cover the range $m_X \leq 50$ MeV and cannot be used to derive a bound for the massless X case.

as the ALP itself, since its mass is set by the same UV scale that suppresses the couplings of the tree-level ALP exchange.

3.2. Lepton Sector

In the lepton sector, the strongest constraints arise from laboratory searches for two-body LFV decays. The decay rates scale with the sum of the squared couplings:

$$\Gamma_{\ell\to\ell' X} \propto |\mathbb{C}^{\mathrm{X}}_{\ell'\ell}|^2 + |\mathbb{C}^{\mathrm{X5}}_{\ell'\ell}|^2. \qquad 10.$$

The experimental difficulty is that these decays look very similar to the corresponding SM decays, resulting in a single visible object plus missing energy. As a consequence, the $\ell \to \ell' X$ decays are not covered by standard LFV searches and require dedicated experimental strategies to suppress the large SM background. One possibility is to study decays of polarized leptons, which yield an angular distribution of the final-state lepton that allows one to distinguish between the chiral LFV couplings because (16, 48)

$$\frac{\mathrm{d}\Gamma(\ell \to \ell' X)}{\mathrm{d}\cos\theta} \propto 1 + 2\cos\theta \cdot \frac{\mathrm{Re}(\mathbb{C}^{\mathrm{X}}_{\ell'\ell}\mathbb{C}^{\mathrm{X5}*}_{\ell'\ell})}{|\mathbb{C}^{\mathrm{X}}_{\ell'\ell}|^2 + |\mathbb{C}^{\mathrm{X5}}_{\ell'\ell}|^2}, \qquad 11.$$

where θ is the angle between the polarization vector of the decaying lepton ℓ and the momentum of the final-state lepton ℓ'. The three-body SM decay rate for final-state lepton energy close to the maximal value $E_{\ell'} = m_\ell/2$ is

$$\frac{\mathrm{d}\Gamma(\ell \to \ell' \nu\bar{\nu})}{\mathrm{d}\cos\theta} \propto 1 - \cos\theta \qquad 12.$$

because of the *V–A* structure of the SM. Therefore, at angles close to $\theta = \pi$ the SM background is strongly reduced, imparting sensitivity to the two-body decay, unless it is aligned with the SM for $\mathbb{C}^{\mathrm{X5}}_{\ell'\ell} = -\mathbb{C}^{\mathrm{X}}_{\ell'\ell}$. The experimental collaborations that search for $\mu \to eX$ usually constrain only a given benchmark scenario, but by using the complete data sets one can constrain any combination of chiral couplings. Here we focus only on the limits of either isotropic decays ($\mathbb{C}^{\mathrm{X}}_{\ell'\ell} = 0$ or $\mathbb{C}^{\mathrm{X5}}_{\ell'\ell} = 0$) or purely left-handed couplings ($\mathbb{C}^{\mathrm{X5}}_{\ell'\ell} = -\mathbb{C}^{\mathrm{X}}_{\ell'\ell}$), and we use the limits obtained by Reference 48 from searches for massless invisible particles in muon decays carried out in the late 1980s at TRIUMF. These limits are severely weakened for couplings aligned with the SM decay and have been replaced by results from TWIST searches that rely on the monochromatic electron as the signal.

Another approach is through three-body decays with an extra photon, $\mu \to e\gamma X$. At present, these decays yield weaker constraints than the two-body decays but show interesting prospects to increase the bound using MEG-II data, as discussed in Section 4. Therefore, we also present the present limit from the Crystal Ball Collaboration (117). Finally, for tau lepton decays, Belle II (100) recently obtained limits on the total branching ratio. **Table 3** summarizes the best current limits on LFV decays. Together with the predictions for the decay rates in References 16 and 48, we use them to derive the limits shown in **Figures 1** and **2**, with a single coupling switched on at a time.

4. FUTURE PROSPECTS

We now review the prospects of future searches for light particles in flavor-violating decays with missing energy. Because of the very different experimental challenges, we again divide the discussion into quark and lepton sectors. In general, the sensitivity can be improved by (*a*) performing existing searches with larger data sets, (*b*) applying dedicated search strategies to existing data sets, and (*c*) performing entirely new searches.

4.1. Quark Sector

Future sensitivities to flavor-violating two-body hadron decays with missing energy can be estimated by rescaling existing searches with the expected luminosity increase. Starting with $K^+ \to \pi^+ X$ and massless X, an improvement by an order of magnitude compared with an older BNL result, $\mathrm{BR}(K^+ \to \pi^+ X) < 7.3 \times 10^{-11}$ (118), can be expected if the full NA62 data set is used (28); we use $\mathrm{BR}_{\mathrm{proj}}(K^+ \to \pi^+ X) = 10^{-11}$ as a conservative projection. KOTO is probing the same flavor transition in a search for the neutral decay mode $K_L \to \pi^0 X$. The KOTO Collaboration (119) expects the sensitivity to be improved down to the 10^{-11} level, which would provide a sensitivity to the *sd* couplings similar to that of NA62. KOTO could also search for the $K_L \to \pi^0 \pi^0 X$, although no feasibility study has been carried out yet. Extending the existing upper limit of the E391a Collaboration (110) on this mode to the case of massless X would lead to the strongest $K \to \pi\pi X$ limit on the *sd* couplings (28).

Another important probe for these transitions is offered by hyperon decays, which already yield the best current limit on axial transitions using searches conducted by BESIII for massless vectors. The present limit of $\mathrm{BR}(\Sigma \to pX) < 3.2 \times 10^{-5}$ already utilizes the full BESIII data set on the J/Ψ resonance, and significant improvements beyond this limit will require a new measurement campaign. For example, a Super Tau Charm Factory (STCF) (124) with an integrated luminosity of 1 ab^{-1} could produce a sample of 3.4×10^{12} J/Ψ particles (~3,400 times more than in BESIII). Our projection for the $\Sigma \to pX$ mode, then, is obtained by rescaling the current bound by the square root of this increase. Future searches for other decay modes such as $\Lambda \to nX$ could reach a similar sensitivity.

Many of the current BESIII bounds on two-body decays probing the *cu* couplings would also be improved by increasing data sets or dedicated searches at a future STCF. For instance, for $D \to \pi X$ decays the situation could easily improve if the two-body analysis were performed over the existing $D^+ \to \tau^+ (\to \pi^+ \bar{\nu}) \nu$ and $D^0 \to \pi^0 \nu \bar{\nu}$ data sets (103, 104, 125). Moreover, the latter analysis employed only 2.93 fb^{-1}, corresponding to a sample of 10^7 $D^0 \bar{D}^0$ pairs. By rescaling the current upper limit on the $D^0 \to \pi^0 \nu \bar{\nu}$ decay (125) by the square root of the ratio of luminosities or number of D^0 mesons, one can forecast the future bounds that could be obtained with the 20 fb^{-1} to be collected by the end of the planned BESIII operation (12), $\mathrm{BR}^{\mathrm{BESIII}}_{\mathrm{proj}}(D^0 \to \pi^0 X) = 8 \times 10^{-5}$, or the 3.6×10^9 $D^0 \bar{D}^0$ pairs to be collected at an STCF (124), $\mathrm{BR}^{\mathrm{STCF}}_{\mathrm{proj}}(D^0 \to \pi^0 X) = 10^{-5}$.

These estimates of the projections for direct searches might be overconservative, as stronger bounds could stem from a dedicated two-body analysis. Therefore, a forecast of charmed baryon decays, where a two-body analysis has been performed with the full BESIII data set, is more direct. Rescaling by the square root of the sample size $\sim 10^5$ Λ_cs reported in the BESIII sample (91) with the 5.6×10^8 charmed baryons planned in an STCF (124), we find $\mathrm{BR}(\Lambda_c \to pX) \lesssim 10^{-6}$. We use this forecast for the projections of the *cu* couplings shown in **Figures 1** and **2**.

For *bs* and *bd* couplings, the sensitivity to branching ratios for invisible decay modes of B mesons will improve significantly with Belle II, where the final integrated luminosity is anticipated to reach 50 ab^{-1}. This increase in luminosity should also enable several dedicated analyses of invisible two-body decays, which will supersede the recasts that are currently used to derive the limits shown in **Table 3**.

To estimate the future sensitivity for the $B \to KX$ transition, we use the recast performed in Reference 97 for the Belle II search for $B^+ \to K^+ \nu \bar{\nu}$ (95), rescaling it by the square root of the ratio of the associated luminosity (362 fb^{-1}) and the prospective size of the data set (50 ab^{-1}). For the rest of the two-body decay modes, we can estimate future limits by similarly rescaling the recasts of the three-body decays reported by BaBar with the corresponding gain in data sample size at Belle II (which is approximately a factor of 100, assuming similar reconstruction efficiencies

at Belle II and BaBar), as done in Reference 28.[4] In the case of $B \to \rho X$, where the only current bound was obtained from a recast of LEP data by Reference 94, the future projection is estimated as in Reference 28, using the current Belle bound on the three-body decay modes $B \to \rho \nu \bar{\nu}$ (for 711 fb^{-1}) (126), but again employing square-root luminosity scaling instead of linear scaling.

Finally, we emphasize that there are several potentially interesting ways to search for a dark boson signal (28). For example, there are no measurements of mesonic decay modes in $c \to u$ transitions that are sensitive to the axial–vector coupling; in other words, there are no $D \to \pi\pi X$ or $D \to \rho X$ searches (where X is an invisible massless particle or dineutrino state). One could also search for a signal in $D_s \to KX$ or $D_s \to K^*X$ decays. All of these searches could be performed at Belle II, BESIII, or STCF.

4.2. Lepton Sector

Probes of SM predictions for rare processes with charged leptons will improve substantially in the next decade. The muon beam experiments MEG-II (15), Mu3e (127, 128), COMET (129), and Mu2e (130) will collect unprecedented data sets using $\mathcal{O}(10^{15}$–$10^{17})$ muons each. Similarly, Belle II and STCF are expected to collect roughly 5×10^{10} (131) and 2×10^{10} (132) $\tau^+\tau^-$ pairs, respectively, exceeding the data sets at Belle and BaBar by more than an order of magnitude.

Starting with two-body tau decays, one can obtain simple estimates for future sensitivities by upscaling the present Belle II bound with the full expected data set, as done in References 48 and 123. Using the current expected bound for BR($\tau \to \ell X$) provided in Reference 100 for 62.8 fb^{-1}, one can estimate that Belle II with 50 ab^{-1} may set 90%-CL limits on flavor-violating tau decays, given by $\text{BR}_{\text{proj}}(\tau \to eX) = 4 \times 10^{-5}$ and $\text{BR}_{\text{proj}}(\tau \to \mu X) = 3 \times 10^{-5}$. Novel analysis strategies have been proposed to further improve signal-to-background discrimination through the use of suitable kinematic variables, which might strengthen these bounds by a factor of three (133) or even by an order of magnitude (134).

Many new ideas have been put forward to increase the sensitivity of searches for two-body muon decays at various muon beam experiments (for a recent proposal for Mu3e searches for $\mu \to eeeX$ and a concise overview of other recent ideas, see Reference 135). The only experimental study to date (120, 121) relies on an online trigger proposal optimized to search for monochromatic $\mu \to eX$ events on top of the three-body SM Michel spectrum at the Mu3e experiment, with an expected limit of $\text{BR}_{\text{proj}}(\mu \to eX)_{\text{iso}} = 7 \times 10^{-8}$. This strategy requires extremely accurate control of theoretical uncertainties because of the irreducible $\mu \to e\bar{\nu}\nu$ background, which was quantified in Reference 136 and implemented in the Monte Carlo code McMule (137).

While the Mu3e approach does not rely on polarization to suppress background and, thus, is independent of the specific chiral structure of dark boson couplings, it faces severe challenges related to systematic uncertainties in searching for a bump close to the endpoint of the SM spectrum (corresponding to massless X), as this region is typically assumed to be signal-free and is used for experimental calibration. For this reason, Mu3e requires alternative calibration techniques and/or search strategies. An interesting proposal in this direction is to look for $\mu \to eeeX$ decays, which can be expected to be sensitive to flavor-violating μe couplings at the same order as the current Mu3e proposal, but without the same experimental challenges.

Another proposal for a new experimental setup at MEG-II is MEG-II-fwd, which would consist of a dedicated calorimeter installed in the forward direction relative to the muon beamline (48). The search strategy, which follows a 1986 experiment by Jodidio et al. (98) that looked for

[4]Note that Reference 28 used an optimistic rescaling linear in the ratio of luminosities, while here we employ a more conservative scaling with the square root of luminosities.

Table 4 Forecast of future laboratory limits on branching ratios of two-body meson, baryon, and lepton decays

Decay[a]	Prospective limit	Experiment[b]
$\mathrm{BR}_{\mathrm{proj}}(K \to \pi X)$	1×10^{-11}	NA62 (28)
$\mathrm{BR}_{\mathrm{proj}}(K \to \pi\pi X)$	7×10^{-7}	E391a (28, 110)
$\mathrm{BR}_{\mathrm{proj}}(\Sigma \to pX)$	2×10^{-6}	STCF
$\mathrm{BR}_{\mathrm{proj}}(D \to \pi X)$	1×10^{-5}	STCF
$\mathrm{BR}_{\mathrm{proj}}(\Lambda_c \to pX)$	1×10^{-6}	STCF
$\mathrm{BR}_{\mathrm{proj}}(B \to KX)$	8×10^{-7}	Belle II
$\mathrm{BR}_{\mathrm{proj}}(B \to K^*X)$	4×10^{-6}	Belle II
$\mathrm{BR}_{\mathrm{proj}}(B \to \pi X)$	2×10^{-6}	Belle II
$\mathrm{BR}_{\mathrm{proj}}(B \to \rho X)$	3×10^{-6}	Belle II
$\mathrm{BR}(\mu \to eX)_{\mathrm{iso}}$	7×10^{-8}	MEG-II-fwd (48)
$\mathrm{BR}(\mu \to eX)_{\mathrm{iso},L,R}$	7×10^{-8}	Mu3e (120, 121)
$\mathrm{BR}(\mu \to eX)_{\mathrm{iso}}$	1×10^{-7}	Mu2e-X, COMET-X (122)
$\mathrm{BR}(\tau \to eX)$	4×10^{-5}	Belle II (48, 123)
$\mathrm{BR}(\tau \to \mu X)$	3×10^{-5}	Belle II (48, 123)

[a] X denotes a massless invisible particle.
[b] The references that performed the forecasts are in parentheses.

$\mu^+ \to e^+ a$ decays, uses the fact that μ^+ is polarized antiparallel to the beam direction, up to depolarization effects. The major benefit of such an experimental setup is that the irreducible SM background from the three-body Michel decay is reduced at the maximal positron momentum $p_{e^+} = m_\mu/2$ in the forward region (in the direction opposite from the polarization of μ^+). Since the SM decay amplitude is controlled by left-handed couplings, it vanishes for an exactly forward positron, if produced from a muon that is completely polarized. For a highly polarized muon beam, the SM background from $\mu^+ \to e^+ \nu \bar{\nu}$ is strongly suppressed in this part of the phase space, while the $\mu^+ \to e^+ a$ decay is allowed for an LFV ALP with nonzero right-handed couplings to the SM leptons. MEG-II-fwd could thus be used to search for an effectively massless ALP produced in $\mu^+ \to e^+ a$, unless its couplings are aligned to the SM (i.e., mainly left-handed): $\mathbb{C}^{\mathrm{X}}_{ij} = -\mathbb{C}^{\mathrm{X5}}_{ij}$. The final reach of MEG-II-fwd depends on how well depolarization effects can be controlled, on the positron momentum resolution of the forward calorimeter, and on whether or not magnetic focusing is applied in order to increase the positron luminosity in the forward direction. **Table 4** shows the expected (optimistic) limit for the isotropic decay $\mathrm{BR}_{\mathrm{proj}}(\mu \to eX)_{\mathrm{iso}} = 7 \times 10^{-8}$ (48).

Another strategy that does not require additional hardware is the MEG-II-ALP proposal for $\mu \to ea\gamma$ (138), which employs an alternative data-taking strategy that would greatly increase the signal acceptance by adjusting the trigger selection while reducing the beam intensity. Indeed, the standard MEG-II trigger is optimized for the $\mu^+ \to e^+\gamma$ decay, as it requires the positron and photon to be back-to-back with equal energies: $E_e = E_\gamma = m_\mu/2$. As a consequence, the trigger is suboptimal for probing $\mu \to ea\gamma$, where the signal rate peaks for a soft photon collinear with the positron. Implementing a new trigger that selects events in this kinematic region would allow MEG-II to search for $\mu^+ \to e^+ a\gamma$ decays, offering a prospective limit on the decay rate that exceeds that of the Crystal Ball Collaboration (117) by more than two orders of magnitude (138).

Finally, the authors of References 122 and 139 have proposed using detector validation data sets of Mu2e to conduct searches for $\mu^+ \to e^+ X$ decays at rest, under the shorthand Mu2e-X. An analogous search (COMET-X) was proposed for the COMET experiment with $\mu^- \to e^- X$ decaying in orbit (140). The projected limit for both proposals is $\mathrm{BR}_{\mathrm{proj}}(\mu \to eX)_{\mathrm{iso}} = 1 \times 10^{-7}$

and, thus, is similar to the reach of Mu3e. However, for massless dark bosons, both the Mu2e and COMET proposals are likely to encounter similar systematic uncertainties as in the $\mu \to eX$ search at Mu3e (135).

5. ASTROPHYSICAL CONSTRAINTS

It is remarkable that flavored dark sectors can also be probed with observations of core-collapse supernovae (SNe), which feature temperatures and densities high enough to sustain a sizable population of moderately heavy flavors. Muons and hyperons are, indeed, expected to emerge in the hot and dense proto–neutron star (PNS) formed during SN explosions (141–144), and could decay into light dark particles carrying energy away from the PNS. This new cooling mechanism can be constrained by observations of SN 1987A (28, 88). Specifically, the duration of the neutrino pulse would have been shorter than observed if the dark luminosity had been comparable to that of the neutrinos (145). These bounds have been extensively explored for muons (48, 146–149) and for hyperons (28, 88, 144, 150, 151).

For hyperons, various models that induce flavor-changing neutral currents, such as $\Lambda \to nX$, have been studied. Focusing on the emission of light dark bosons, one can estimate the energy loss rate per unit volume Q as the product of the hyperon number density n_Λ (the energy released per decay, given approximately by the hyperon–neutron mass difference) and the hyperon decay rate, yielding $Q \propto n_\Lambda (m_\Lambda - m_n)\Gamma(\Lambda \to nX)$. One can then approximately describe the effects of neutron degeneracy (28, 145) by a single number F_n, given by the thermal average of the Pauli blocking factor (145). An estimate of the emissivity (the energy loss rate per unit mass) ϵ in the nonrelativistic limit, then, is

$$\epsilon \approx F_n Y_\Lambda \frac{m_\Lambda - m_n}{m_n} \frac{\mathrm{BR}(\Lambda \to nX)}{\tau_\Lambda}, \qquad 13.$$

where τ_Λ is the hyperon lifetime and $Y_\Lambda = n_\Lambda / n_B$ is the abundance of hyperons in the PNS, normalized by the baryonic number density. By adopting the classical upper limit on emissivity, $\epsilon_{\max} = 10^{19}\ \mathrm{erg\ s^{-1}\ g^{-1}}$ (145), from SN 1987A under the conditions predicted for the PNS around 1 s postbounce, one obtains

$$\epsilon \approx \epsilon_{\max} \left(\frac{Y_\Lambda}{0.01}\right)\left(\frac{0.7}{F_n}\right)\left(\frac{2 \times 10^{-9}}{\mathrm{BR}(\Lambda \to nX)}\right). \qquad 14.$$

Therefore, for a typical Λ abundance of 1%, the upper limit on the branching fraction is in the range of 10^{-9}, which is many orders of magnitude more stringent than the limits obtained from laboratory searches, for example, with the full data set at BESIII (see Section 4.1).

Furthermore, as discussed in Reference 88, excessive emission of dark bosons from hyperon decays would still occur in the deep-trapping regime (corresponding to large couplings or large branching fractions). The reason is that the dark luminosity would have to originate from the surface, where Λs remain in equilibrium with the plasma, which corresponds to a high-temperature region.

The estimate in Equation 14 has been improved with a complete calculation of the decay process using kinetic theory, including the effects of the medium on the dispersion relation of the baryons (88). Moreover, radial profiles of all the thermodynamical quantities relevant for the calculations of the rates can be extracted from spherically symmetric simulations, such as those reported in Reference 146, that are designed for these types of studies. These simulations did not include hyperons in the nuclear equation of state or the feedback of the energy loss caused by the invisible decays of the Λ in the SN simulation. Nonetheless, Reference 88 derived upper limits on the branching ratio and recalculated the thermodynamic quantities at 1 s postbounce by using

interpolation tables based on hyperonic extensions of the equation of state used in the simulations. The upper limit thus obtained is

$$\mathrm{BR}(\Lambda \to nX) \lesssim 8 \times 10^{-9}, \tag{15.}$$

which is the weakest among those obtained via the different simulations reported in Reference 146. This result is weaker than the approximate expression in Equation 14 by a factor of ∼4, which translates into a factor of ∼2 weaker bound on the UV scale of the dark boson. For scalar couplings, these bounds are $\Lambda_{\mathrm{eff}} \gtrsim 7 \times 10^9$ GeV and $\Lambda_{\mathrm{eff}} \gtrsim 5 \times 10^9$ GeV for $\mathbb{C}^{\mathrm{S}}_{sd}$ and $\mathbb{C}^{\mathrm{S5}}_{sd}$, respectively, and $\Lambda_{\mathrm{eff}} \gtrsim 1 \times 10^{10}$ GeV for the massless vector with dipole couplings.

Reference 152 reported the first simulations incorporating a hyperonic equation of state and energy losses due to invisible Λ decays. These simulations demonstrate that such decays accelerate deleptonization of the PNS and enhance cooling, reducing the neutrino emission timescale by a factor of two and thereby validating previous analyses.

A similar analysis can be performed for the LFV muon decay $\mu \to eX$. Using the same approximations as for hyperons, one would find for this process an equation analogous to Equation 13 with the appropriate replacements [i.e., $\delta \to (m_\mu - m_e)/m_n$]. Thus, for muon decays one obtains

$$\epsilon \approx \epsilon_{\max} \left(\frac{Y_\mu}{0.03}\right)\left(\frac{0.5}{F_n}\right)\left(\frac{10^{-5}}{\mathrm{BR}(\mu \to eX)}\right), \tag{16.}$$

which, contrary to the case of the quark couplings and the hyperon decays, is a bound much weaker than those obtained from laboratory experiments (for a related analysis that uses different production processes but obtains similar limits, see Reference 153).

Finally, we comment on astrophysical limits on flavor-diagonal couplings to fermions, which can be compared with the limits on flavor violation. If we write the scalar couplings to electrons and neutrons as $\mathcal{L} = -a/\Lambda[m_e \bar{e}(\mathbb{C}^{\mathrm{S}}_{ee} + \mathbb{C}^{\mathrm{S5}}_{ee}\gamma_5]e + m_N \overline{N}(\mathbb{C}^{\mathrm{S}}_{NN} + \mathbb{C}^{\mathrm{S5}}_{NN}\gamma_5)N$, then the star cooling limits from red giants (RGs) yield $\Lambda/\mathbb{C}^{\mathrm{S}}_{ee,NN} \gtrsim 7 \times 10^{11}$ GeV (154) and a recent analysis of the white dwarf (WD) luminosity function yields $\Lambda/\mathbb{C}^{\mathrm{S}}_{ee,NN} \gtrsim 1 \times 10^{12}$ GeV (155), with only small differences between electrons and nucleons. Limits on couplings to pseudoscalar currents are weaker, with $\Lambda/\mathbb{C}^{\mathrm{S5}}_{ee} \gtrsim 2 \times 10^9$ GeV from WDs (156) and $\Lambda/\mathbb{C}^{\mathrm{S5}}_{NN} \gtrsim 8 \times 10^8$ GeV from SN 1987A (157). Note that for light vectors with diagonal couplings of the form in Equation 2 and derivatively coupled scalars (Equation 6), the latter bounds apply. Even the most stringent limits on scalar couplings are surpassed by laboratory limits on $s \to d$ transitions, with the potential to be extended in the near future by NA62. In contrast, star cooling limits on pseudoscalar diagonal couplings to nucleons and electrons (including couplings of light vectors and derivatively coupled axions) are at the level of 10^9 GeV, which is comparable to present limits on $\mu \to e$ transitions and prospects on $b \to s$ and $b \to d$ transitions. We emphasize that the bounds from star cooling of RGs (WDs) are not valid for dark boson masses above the typical core temperatures of approximately 10 keV (1 keV), while the laboratory limits discussed in the previous sections extend to much larger masses.

6. COSMOLOGICAL CONSTRAINTS

Since DM is our main motivation to look for missing energy in flavor-violating decays, we discuss their impact in cosmological scenarios where the dark boson is directly connected to the DM abundance. In this section, we describe these aspects in more detail. The simplest possibility is that the boson is stable even on cosmological scales and is produced in the early Universe in quantities that amount to the observed relic DM abundance: $\Omega_{\mathrm{DM}}h^2 = 0.12$. The preferred production mechanism depends crucially on the dark boson mass: Very light bosons with masses well below the keV scale have to be nonthermally produced in order to avoid constraints on warm

DM (WDM). A classic production mechanism of this kind is misalignment, which was originally proposed for the QCD axion (25–27) and then generalized for generally light feebly interacting bosons (63). However, a thermal population of such light particles can also be produced by the flavor-violating interactions in Equation 4, which are then subject to stringent constraints on dark radiation and WDM. If this production channel dominates over misalignment, it can fully account for the observed DM abundance via thermal freeze-in (52). This possibility allows for a direct link between the size of flavor-violating decay rates and the DM relic abundance.

6.1. Constraints from Dark Radiation

While misalignment can easily yield light bosons behaving as cold DM in the required quantities, such particles can also be produced thermally by direct couplings to SM particles and are relativistic at least at the early stage of evolution of the Universe (158). In the context of flavor-violating interactions in Equation 4, the main production channel would be through decays of SM fermions. For sufficiently large couplings (sufficiently small $\Lambda/\mathbb{C}_{ij}$), such decays (and their inverse processes) bring the light bosons into thermal equilibrium with the SM plasma. When the temperature drops, the rate of inverse processes peters out, and the dark bosons maintain their freeze-out abundance when they decouple from the thermal bath. Alternatively, when the couplings are so small that thermal equilibrium is never achieved, a dark boson abundance slowly builds up from SM fermion decays until the temperature drops below the mass of the mother fermion, so that it becomes nonrelativistic and its abundance is exponentially suppressed.

Thermal relics are constrained by big bang nucleosynthesis, observations of the cosmic microwave background (CMB), and structure formation. Very light (sub-eV) particles such as the QCD axion are relativistic at recombination and, thus, contribute to dark radiation (e.g., to the energy density stored in relativistic degrees of freedom), which is conveniently parameterized in terms of the effective number of additional neutrino species $\Delta N_{\rm eff}$. This observable is constrained by CMB observations and baryon acoustic oscillations, and the most recent combined analysis by the Planck Collaboration (159) set the upper bound $\Delta N_{\rm eff} \leq 0.3$ at 95% CL. This bound is expected to be improved to 0.1 at the Simons Observatory (160) and eventually to 0.05 by the CMB-S4 experiment (161).

These limits allow one to constrain flavor-violating couplings of very light bosons provided that they are stable not only on collider but also on cosmological scales, which requires a calculation of their energy density at the time of recombination. The resulting constraints have been studied (123, 162–165), and we report the results below.

Starting with LFV transitions, current laboratory limits on muon decays are stronger than the projected CMB-S4 bound from cosmology, yielding $\Lambda_{\rm eff} \gtrsim 10^9$ GeV for $\mu \to e$ transitions (165). Instead, for $\tau \to \ell$ transitions (there is essentially no difference between $\ell = \mu$ and $\ell = e$), the projected limit is of the order of 10^8 GeV (123) and the present bound from Planck cannot compete with the current Belle II limit (according to Reference 166, which refined the calculation in Reference 165 that suggested the opposite conclusion).

In the quark sector, the NA62 limits on $s \to d$ far exceed even future cosmology projections (165). In contrast, the CMB-S4 projections for $b \to s, d$ transitions are of order $\Lambda_{\rm eff} \gtrsim 10^8$ GeV (164), which, interestingly, are in the same ballpark as the projected limits for Belle II. Note that Reference 165 found more stringent cosmology limits; however, it is not entirely clear whether the production rates from flavor-violating scattering processes were appropriately treated, given the complications from IR divergencies that could contribute large unphysical enhancement factors (167). For the same reason, their projection on $c \to u$ transitions might be too optimistic. One can obtain a more conservative estimate by using the result in

Reference 162 (which takes into account only decays) to find $\Lambda_{\rm eff} \gtrsim 10^8$ GeV, which, again, is at the same level of the BESIII and STCF projections. We emphasize that these limits from $\Delta N_{\rm eff}$ are invalidated (*a*) if the dark boson is sufficiently heavy to avoid constraints from dark radiation and WDM (i.e., for roughly $m_X \gtrsim$ few keV), (*b*) if the boson is stable only on collider and not cosmological scales, or (*c*) if sizable couplings to SM particles substantially alter the dark boson's thermal history.

6.2. Dark Matter Relic Abundance

For dark bosons with masses above a few keV, the $\Delta N_{\rm eff}$ and WDM bounds can be avoided, and one can consider scenarios where the flavor-violating decays are in fact the dominant production of light bosonic DM, reproducing the observed DM abundance via thermal freeze-in (52). The relic abundance is then set by the product of the DM mass, m_X, and the flavor-violating decay rate, $\Omega_X h^2 \propto m_X \Gamma(f_i \to f_j X) \propto m_X (\mathbb{C}_{ij}^{X,X5}/\Lambda)^2$, yielding a prediction for the decay rate as a function of the dark boson mass. Such a determination of the decay rate otherwise requires extensive flavor model building (see Section 2). This kind of scenario serves as a possible motivation for explicit experimental targets, directly connecting the flavor-violating decays to the DM abundance. Therefore, we provide some details of these models below, focusing on the case of ALPs discussed in References 167 and 168.

The main challenge of this scenario is DM stability, as the ALP can always decay into two photons at a decay rate set by

$$\Gamma_{a\to\gamma\gamma} \approx \frac{\alpha_{\rm em}^2}{64\pi^3}\frac{m_a^3}{f_a^2}\left|C_\gamma\right|^2, \qquad C_\gamma = E - 1.92N + \sum_i C_{ii}^A \frac{m_a^2}{12 m_i^2}, \tag{17.}$$

up to higher powers of m_a^2/m_i^2 and where the sum runs over all electrically charged SM fermions. Here, C_{ii}^A are the diagonal axion couplings to fermions in Equation 6 and $E(N)$ are the electromagnetic (color) anomaly coefficients of the model, determined by the fermion couplings. Although it is relatively easy to make the axion lifetime larger than the age of the Universe, $1/H_0 \sim 10^{17}$ s, it turns out that, in the relevant axion mass range, much stronger constraints on the decay rate arise from X-ray telescopes, requiring $\Gamma_{a\to\gamma\gamma} \gtrsim 10^{28}$ s (168). This requirement implies that the underlying PQ symmetry must be anomaly-free, and one needs $m_a \ll m_i$ and/or $C_{ii}^A \ll C_{ij}^{A,V}$. In fact, note that DM production is controlled by $C_{i\neq j}^{A,V}$ while DM stability is governed by C_{ii}^A, so in principle these are independent parameters, although a strong hierarchy $C_{ii}^A \ll C_{ij}^{A,V}$ seems unnatural. In any case, ALP stability yields an upper bound on m_a, while a lower bound arises from experimental limits on the decay rate [since $\Omega_a h^2 \propto m_a \Gamma(f_i \to f_j a)$] and from Lyman-α limits on WDM, which in the case of freeze-in production require $m_a \gtrsim 10$ keV.

As an explicit example, we consider the effective two-flavor scenario discussed in Reference 168, where two right-handed SM leptons are oppositely charged under PQ and a single angle parameterizes the rotation to the mass basis. This simplified model has only three parameters: the axion mass m_a; the axion decay constant f_a; and a single angle $0 \le \alpha \le \pi/2$, which controls the couplings to leptons, for example, for the μe scenario

$$C_{ee}^A = -C_{\mu\mu}^A = \sin\alpha, \qquad C_{\mu e}^A = C_{\mu e}^V = \cos\alpha. \tag{18.}$$

After fixing the axion decay constant to reproduce the observed abundance, one is left with a two-dimensional parameter space, where constraints on decaying DM, WDM, and direct laboratory searches are imposed (**Figure 3**). The stringent bounds from X-ray searches require diagonal axion couplings to be smaller than off-diagonal ones by at least 1%, ruling out the limit of exact flavor conservation $\alpha = \pi/2$. Present limits from laboratory searches are roughly at the same level as

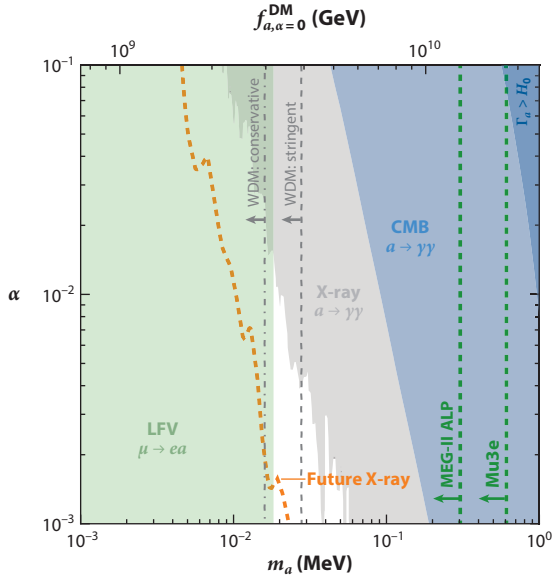

Figure 3

Allowed parameter space for dark matter (DM) freeze-in through lepton flavor–violating (LFV) decays (168). The axion-like particle (ALP) decay constant f_a (top x axis) is determined by requiring that the DM abundance today be produced through freeze-in, once the ALP mass m_a (bottom x axis) and the mixing angle α are fixed, as defined in Equation 18 (we choose the reference value $\alpha = 0$). The dark blue shaded, blue shaded, and gray shaded regions are excluded by the DM lifetime, cosmic microwave background (CMB), and X-ray constraints on decaying DM, respectively. The dashed orange line represents the reach of future X-ray searches. Dash-dotted (dashed) gray lines represent conservative (stringent) constraints on warm dark matter (WDM) requiring $m_{\mathrm{WDM}} \gtrsim 3.5$ (5.3) keV. The green shaded region indicates the present bound from $\mu \to ea$ searches, and dashed green lines represent the prospects for future proposed searches at MEG-II (138) and Mu3e (48, 120). Figure adapted from Reference 168 (CC BY 4.0).

WDM constraints, but the proposed searches at MEG-II and Mu3e will probe almost the entire allowed parameter space. These experiments offer the unique opportunity to probe directly the very same decay that could have produced axion DM in the early Universe.

SUMMARY POINTS

1. Flavor-violating decays with light invisible states, mimicking Standard Model (SM) three-body decays with neutrino pairs, can be probed at colliders. In contrast to heavy new physics contributions, these searches are controlled by dimension-five operators and thus provide exceptional sensitivity to high-energy scales, with current limits ranging from 10^7 GeV (tau and charm) to nearly 10^{12} GeV (kaons).
2. Light dark bosons with flavor-violating couplings have decent theoretical motivation via the strong *CP* problem, the dark matter (DM) relic abundance, and/or the SM flavor puzzle, for example, as QCD axions of a flavor-nonuniversal Peccei–Quinn symmetry.
3. Muons and hyperons are present in proto–neutron stars formed during core-collapse supernovae (SNe). Their decays into invisible states introduce a new cooling mechanism

constrained by SN 1987A. The resulting limits on hyperon decays are stronger than those from laboratory experiments by several orders of magnitude.

4. Flavor-violating decays can take place in the early Universe, producing a relic abundance of light dark states. While DM masses below a few keV are constrained by dark radiation and warm DM limits, heavier bosons could account for the observed DM abundance with a direct link to the size of flavor-violating couplings.

FUTURE ISSUES

1. Flavor constraints on light dark sectors could be strengthened considerably by improving existing searches with larger data sets, applying dedicated analysis strategies to current data, or conducting entirely new searches.
2. Projected sensitivities to the UV scale exceed 10^{12} GeV in kaon decays (NA62), 10^{10} GeV in muon decays (Mu3e and MEG-II), and 10^{8} GeV in *B* meson (Belle II) and charmed hadron decays (BESIII and STCF).
3. Predictions of flavor-violating couplings in explicit models are rare. Their determination in motivated SM extensions will prove valuable in defining explicit experimental targets for probing dark-flavored sectors.
4. In many cases, there is an interesting interplay between future collider and cosmological constraints, which motivates a more precise assessment of prospective collider limits and DM production rates in the early Universe.

DISCLOSURE STATEMENT

The authors are not aware of any affiliations, memberships, funding, or financial holdings that might be perceived as affecting the objectivity of this review.

ACKNOWLEDGMENTS

J.M.C. thanks MICINN for funding through the grant "DarkMaps" (PID2022-142142NB-I00) and through the European Union grant "UNDARK" from the Widening Participation and Spreading Excellence program (project number 101159929). The writing of this review received support from the European Union's Horizon 2020 research and innovation program under a Marie Skłodowska-Curie grant (860881-HIDDeN) and was partially supported by projects B3a and C3b of the DFG-funded Collaborative Research Center (TRR257, "Particle Physics Phenomenology after the Higgs Discovery"). R.Z. thanks the INFN National Laboratory of Frascati, where this review was partially written, for its kind hospitality.

LITERATURE CITED

1. Knapen S, Lin T, Zurek KM. *Phys. Rev. D* 96:115021 (2017)
2. Lin T. *Proc. Sci*. TASI2018:009 (2019)
3. Zurek KM. *Annu. Rev. Nucl. Part. Sci.* 74:287 (2024)
4. Cirelli M, Strumia A, Zupan J. arXiv:2406.01705 [hep-ph] (2024)
5. Wilczek F. *Phys. Rev. Lett.* 49:1549 (1982)
6. Holdom B. *Phys. Lett. B* 166:196 (1986)

7. Dobrescu BA. *Phys. Rev. Lett.* 94:151802 (2005)
8. Elor G, Escudero M, Nelson A. *Phys. Rev. D* 99:035031 (2019)
9. Kamenik JF, Smith C. *J. High Energy Phys.* 1203:090 (2012)
10. Aaij R, et al. arXiv:1808.08865 [hep-ex] (2018)
11. Altmannshofer W, et al. *Prog. Theor. Exp. Phys.* 2019:123C01 (2019). Erratum. *Prog. Theor. Exp. Phys.* 2020:029201 (2020)
12. Ablikim M, et al. *Chin. Phys. C* 44:040001 (2020)
13. Cortina Gil E, et al. *J. Instrum.* 12:P05025 (2017)
14. Yamanaka T. *Prog. Theor. Exp. Phys.* 2012:02B006 (2012)
15. Baldini AM, et al. *Eur. Phys. J. C* 78(5):380 (2018)
16. Eguren JF, Klingel S, Stamou E, Tabet M, Ziegler R. *J. High Energy Phys.* 2408:111 (2024)
17. Fabbrichesi M, Gabrielli E, Mele B. *Phys. Rev. Lett.* 119:031801 (2017)
18. Di Luzio L, Giannotti M, Nardi E, Visinelli L. *Phys. Rep.* 870:1 (2020)
19. Feruglio F. *Eur. Phys. J. C* 75(8):373 (2015)
20. Wilczek F. *Phys. Rev. Lett.* 40:279 (1978)
21. Weinberg S. *Phys. Rev. Lett.* 40:223 (1978)
22. Peccei RD, Quinn HR. *Phys. Rev. Lett.* 38:1440 (1977)
23. Peccei RD, Quinn HR. *Phys. Rev. D* 16:1791 (1977)
24. Grilli di Cortona G, Hardy E, Pardo Vega J, Villadoro G. *J. High Energy Phys.* 1601:034 (2016)
25. Preskill J, Wise MB, Wilczek F. *Phys. Lett. B* 120:127 (1983)
26. Abbott LF, Sikivie P. *Phys. Lett. B* 120:133 (1983)
27. Dine M, Fischler W. *Phys. Lett. B* 120:137 (1983)
28. Martin Camalich J, et al. *Phys. Rev. D* 102:015023 (2020)
29. Kim JE. *Phys. Rev. Lett.* 43:103 (1979)
30. Shifman MA, Vainshtein AI, Zakharov VI. *Nucl. Phys. B* 166:493 (1980)
31. Dine M, Fischler W, Srednicki M. *Phys. Lett. B* 104:199 (1981)
32. Zhitnitsky AR. *Sov. J. Nucl. Phys.* 31:260 (1980)
33. Bardeen WA, Peccei RD, Yanagida T. *Nucl. Phys. B* 279:401 (1987)
34. Geng CQ, Ng JN. *Phys. Rev. D* 39:1449 (1989)
35. Hindmarsh M, Moulatsiotis P. *Phys. Rev. D* 56:8074 (1997)
36. Di Luzio L, et al. *Phys. Rev. Lett.* 120:261803 (2018)
37. Björkeroth F, et al. *Phys. Rev. D* 101:035027 (2020)
38. Saikawa K, Yanagida TT. *J. Cosmol. Astropart. Phys.* 2003:007 (2020)
39. Badziak M, Grilli di Cortona G, Tabet M, Ziegler R. *J. High Energy Phys.* 2110:181 (2021)
40. Davidson A, Wali KC. *Phys. Rev. Lett.* 48:11 (1982)
41. Berezhiani ZG, Khlopov MY. *Z. Phys. C* 49:73 (1991)
42. Ema Y, Hamaguchi K, Moroi T, Nakayama K. *J. High Energy Phys.* 1701:096 (2017)
43. Calibbi L, et al. *Phys. Rev. D* 95:095009 (2017)
44. Froggatt CD, Nielsen HB. *Nucl. Phys. B* 147:277 (1979)
45. Ibanez LE, Ross GG. *Phys. Lett. B* 332:100 (1994)
46. Binetruy P, Ramond P. *Phys. Lett. B* 350:49 (1995)
47. Linster M, Ziegler R. *J. High Energy Phys.* 1808:058 (2018)
48. Calibbi L, Redigolo D, Ziegler R, Zupan J. *J. High Energy Phys.* 2109:173 (2021)
49. Choi K, Im SH, Park CB, Yun S. *J. High Energy Phys.* 1711:070 (2017)
50. Chala M, Guedes G, Ramos M, Santiago J. *Eur. Phys. J. C* 81(2):181 (2021)
51. Bauer M, et al. *J. High Energy Phys.* 2209:056 (2022)
52. Hall LJ, Jedamzik K, March-Russell J, West SM. *J. High Energy Phys.* 1003:080 (2010)
53. Co RT, Hall LJ, Harigaya K. *Phys. Rev. Lett.* 120:211602 (2018)
54. Greljo A, Smolkovič A, Valenti A. *J. High Energy Phys.* 2409:174 (2024)
55. Heeck J. *Phys. Lett. B* 813:136043 (2021)
56. Chikashige Y, Mohapatra RN, Peccei RD. *Phys. Lett. B* 98:265 (1981)
57. Schechter J, Valle JWF. *Phys. Rev. D* 25:774 (1982)

58. Cicoli M. In *Proceedings, 9th Patras Workshop on Axions, WIMPs and WISPs*, ed. U Oberlack, P Sissol. DESY (2013)
59. Feruglio F, Ziegler R. arXiv:2411.08101 [hep-ph] (2024)
60. Feruglio F. In *From My Vast Repertoire... Guido Altarelli's Legacy*, ed. S Forte, A Levy, G Ridolfi. World Scientific (2019)
61. Feruglio F, Strumia A, Titov A. *J. High Energy Phys.* 2307:027 (2023)
62. Nelson AE, Scholtz J. *Phys. Rev. D* 84:103501 (2011)
63. Arias P, et al. *J. Cosmol. Astropart. Phys.* 1206:013 (2012)
64. Smolkovič A, Tammaro M, Zupan J. *J. High Energy Phys.* 1910:188 (2019). Erratum. *J. High Energy Phys.* 2202:033 (2022)
65. Bonnefoy Q, Dudas E, Pokorski S. *J. High Energy Phys.* 2001:191 (2020)
66. Greljo A, Thomsen AE. *Eur. Phys. J. C* 84(2):213 (2024)
67. Foot R, He XG, Lew H, Volkas RR. *Phys. Rev. D* 50:4571 (1994)
68. Ardu M, Kirk F. *Eur. Phys. J. C* 83(5):394 (2023)
69. Grinstein B, Redi M, Villadoro G. *J. High Energy Phys.* 1011:067 (2010)
70. Fabbrichesi M, Gabrielli E, Lanfranchi G. arXiv:2005.01515 [hep-ph] (2020)
71. Patt B, Wilczek F. arXiv:hep-ph/0605188 (2006)
72. Batell B, Pospelov M, Ritz A. *Phys. Rev. D* 80:095024 (2009)
73. Lanfranchi G, Pospelov M, Schuster P. *Annu. Rev. Nucl. Part. Sci.* 71:279 (2021)
74. Alekhin S, et al. *Rep. Prog. Phys.* 79:124201 (2016)
75. Anelli M, et al. arXiv:1504.04956 [physics.in-det] (2015)
76. Feng JL, Galon I, Kling F, Trojanowski S. *Phys. Rev. D* 97:035001 (2018)
77. Ariga A, et al. arXiv:1812.09139 [physics.in-det] (2018)
78. Döbrich B, Ertas F, Kahlhoefer F, Spadaro T. *Phys. Lett. B* 790:537 (2019)
79. Balkin R, Burger N, Feng JL, Shadmi Y. arXiv:2412.15197 [hep-ph] (2024)
80. Feng JL, Moroi T, Murayama H, Schnapka E. *Phys. Rev. D* 57:5875 (1998)
81. Björkeroth F, Chun EJ, King SF. *J. High Energy Phys.* 1808:117 (2018)
82. Carmona A, Scherb C, Schwaller P. *J. High Energy Phys.* 2108:121 (2021)
83. Ibarra A, Marín M, Roig P. *Phys. Lett. B* 827:136933 (2022)
84. Heeck J. *Phys. Lett. B* 758:101 (2016)
85. Gabrielli E, Mele B, Raidal M, Venturini E. *Phys. Rev. D* 94:115013 (2016)
86. Su JY, Tandean J. *Phys. Rev. D* 101:035044 (2020)
87. Su JY, Tandean J. *Eur. Phys. J. C* 80(9):824 (2020)
88. Camalich JM, Terol-Calvo J, Tolos L, Ziegler R. *Phys. Rev. D* 103:L121301 (2021)
89. Cortina Gil E, et al. *J. High Energy Phys.* 2106:093 (2021)
90. Ablikim M, et al. *Phys. Lett. B* 852:138614 (2024)
91. Ablikim M, et al. *Phys. Rev. D* 106:072008 (2022)
92. Aubert B, et al. *Phys. Rev. Lett.* 94:101801 (2005)
93. Barate R, et al. *Eur. Phys. J. C* 19:213 (2001)
94. Alonso-Álvarez G, Escudero Abenza M. *Eur. Phys. J. C* 84(5):553 (2024)
95. Adachi I, et al. *Phys. Rev. D* 109:112006 (2024)
96. Lees JP, et al. *Phys. Rev. D* 87:112005 (2013)
97. Altmannshofer W, et al. *Phys. Rev. D* 109:075008 (2024)
98. Jodidio A, et al. *Phys. Rev. D* 34:1967 (1986). Erratum. *Phys. Rev. D* 37:237 (1988)
99. Bayes R, et al. *Phys. Rev. D* 91:052020 (2015)
100. Adachi I, et al. *Phys. Rev. Lett.* 130:181803 (2023)
101. Eisenstein BI, et al. *Phys. Rev. D* 78:052003 (2008)
102. Guadagnoli D, et al. arXiv:2503.05865 [hep-ph] (2025)
103. Ablikim M, et al. *Phys. Rev. Lett.* 123:211802 (2019)
104. Ablikim M, et al. arXiv:2410.20063 [hep-ex] (2024)
105. Ablikim M, et al. *Phys. Rev. D* 111:L011103 (2025)
106. Su JY, Tandean J. *Phys. Rev. D* 102:115029 (2020)

107. Albrecht J, Stamou E, Ziegler R, Zwicky R. *J. High Energy Phys.* 2021:139 (2020)
108. Adler S, et al. *Phys. Rev. D* 63:032004 (2001)
109. Sadovsky AS, et al. *Eur. Phys. J. C* 84(3):266 (2024)
110. Ogata R, et al. *Phys. Rev. D* 84:052009 (2011)
111. Batley JR, et al. *Eur. Phys. J. C* 70:635 (2010)
112. Batley JR, et al. *Phys. Lett. B* 715:105 (2012). Addendum. *Phys. Lett. B* 740:364 (2015)
113. Littenberg LS, Valencia G. *Phys. Lett. B* 385:379 (1996)
114. Chiang CW, Gilman FJ. *Phys. Rev. D* 62:094026 (2000)
115. Cavan-Piton M, et al. arXiv:2411.04170 [hep-ph] (2024)
116. Bona M, et al. *Proc. Sci.* WIFAI2023:007 (2024)
117. Bolton RD, et al. *Phys. Rev. D* 38:2077 (1988)
118. Adler S, et al. *Phys. Rev. D* 77:052003 (2008)
119. Goudzovski E, et al. *Rep. Prog. Phys.* 86:016201 (2023)
120. Perrevoort AK. *SciPost Phys. Proc.* 1:052 (2019)
121. Perrevoort AK. *Sensitivity studies on new physics in the Mu3e experiment and development of firmware for the front-end of the Mu3e pixel detector*. PhD Thesis, University of Heidelberg (2018)
122. Hill RJ, Plestid R, Zupan J. *Phys. Rev. D* 109:035025 (2024)
123. Badziak M, Harigaya K, Łukawski M, Ziegler R. *J. High Energy Phys.* 2409:136 (2024)
124. Zhou X. *Proc. Sci*. CHARM2020:007 (2021)
125. Ablikim M, et al. *Phys. Rev. D* 105:L071102 (2022)
126. Grygier J, et al. *Phys. Rev. D* 96:091101 (2017). Addendum. *Phys. Rev. D* 97:099902 (2018)
127. Berger N. *Nucl. Phys. B* 248–250:35 (2014)
128. Blondel A, et al. arXiv:1301.6113 [physics.ins-det] (2013)
129. Abramishvili R, et al. *Prog. Theor. Exp. Phys.* 2020:033C01 (2020)
130. Bartoszek L, et al. arXiv:1501.05241 [physics.ins-det] (2014)
131. Rodríguez Pérez D. arXiv:1906.08950 [hep-ex] (2019)
132. Achasov M, et al. *Front. Phys.* 19:14701 (2024)
133. Guadagnoli D, Park CB, Tenchini F. *Phys. Lett. B* 822:136701 (2021)
134. De La Cruz-Burelo E, Hernandez-Villanueva M, De Yta-Hernandez A. *Phys. Rev. D* 102:115001 (2020)
135. Knapen S, Langhoff K, Opferkuch T, Redigolo D. arXiv:2311.17915 [hep-ph] (2023)
136. Banerjee P, et al. *SciPost Phys*. 15:021 (2023)
137. Banerjee P, Engel T, Signer A, Ulrich Y. *SciPost Phys.* 9:027 (2020)
138. Jho Y, Knapen S, Redigolo D. *J. High Energy Phys.* 2210:029 (2022)
139. Huang S. *Search for lepton flavor violation in two body muon and pion decay at rest*. PhD Thesis, Purdue University (2022)
140. Xing T, et al. *Chin. Phys. C* 47:013108 (2023)
141. Ambartsumyan VA, Saakyan GS. *Sov. Astron.* 4:187 (1960)
142. Oertel M, Hempel M, Klähn T, Typel S. *Rev. Mod. Phys.* 89:015007 (2017)
143. Bollig R, et al. *Phys. Rev. Lett.* 119:242702 (2017)
144. Fischer T, et al. *Phys. Rev. D* 102:123001 (2020)
145. Raffelt GG. *Stars as Laboratories for Fundamental Physics: The Astrophysics of Neutrinos, Axions, and Other Weakly Interacting Particles*. University of Chicago Press (1996)
146. Bollig R, DeRocco W, Graham PW, Janka HT. *Phys. Rev. Lett.* 125:051104 (2020). Erratum. *Phys. Rev. Lett.* 126:189901 (2021)
147. Croon D, Elor G, Leane RK, McDermott SD. *J. High Energy Phys.* 2101:107 (2021)
148. Caputo A, Raffelt G, Vitagliano E. *Phys. Rev. D* 105:035022 (2022)
149. Manzari CA, Martin Camalich J, Spinner J, Ziegler R. *Phys. Rev. D* 108:103020 (2023)
150. Alonso-Álvarez G, et al. *Phys. Rev. D* 105:115005 (2022)
151. Cavan-Piton M, et al. *Phys. Rev. Lett.* 133:121002 (2024)
152. Fischer T, Martin Camalich J, Kochankovski H, Tolos L. arXiv:2408.01406 [astro-ph.HE] (2024)
153. Zhang HY, Hagimoto R, Long AJ. *Phys. Rev. D* 109:103005 (2024)
154. Hardy E, Lasenby R. *J. High Energy Phys.* 1702:033 (2017)

155. Bottaro S, Caputo A, Raffelt G, Vitagliano E. *J. Cosmol. Astropart. Phys.* 2307:071 (2023)
156. Miller Bertolami MM, Melendez BE, Althaus LG, Isern J. *J. Cosmol. Astropart. Phys.* 1410:069 (2014)
157. Carenza P, et al. *J. Cosmol. Astropart. Phys.* 1910:016 (2019). Erratum. *J. Cosmol. Astropart. Phys.* 2005:E01 (2020)
158. Chang S, Choi K. *Phys. Lett. B* 316:51 (1993)
159. Aghanim N, et al. *Astron. Astrophys.* 641:A6 (2020). Erratum. *Astron. Astrophys.* 652:C4 (2021)
160. Ade P, et al. *J. Cosmol. Astropart. Phys.* 1902:056 (2019)
161. Abazajian KN, et al. arXiv:1610.02743 [astro-ph.CO] (2016)
162. Baumann D, Green D, Wallisch B. *Phys. Rev. Lett.* 117:171301 (2016)
163. D'Eramo F, Ferreira RZ, Notari A, Bernal JL. *J. Cosmol. Astropart. Phys.* 1811:014 (2018)
164. Arias-Aragón F, et al. *J. Cosmol. Astropart. Phys.* 2103:090 (2021)
165. D'Eramo F, Yun S. *Phys. Rev. D* 105:075002 (2022)
166. Badziak M, Laletin M. *J. High Energy Phys.* 02:108 (2025)
167. Aghaie M, et al. *Phys. Lett. B* 856:138923 (2024)
168. Panci P, Redigolo D, Schwetz T, Ziegler R. *Phys. Lett. B* 841:137919 (2023)